Numerical Simulation and Experimental Verification of Temperature Distribution of Piezoelectric Stack with Heating and Thermal Insulation Device

CHEN Yixiao[1,3], *YANG Xinghua*[2*], *YU Li*[2], *SHEN Xing*[1]

1. State Key Laboratory of Mechanics and Control of Mechanical Structures, Nanjing University of Aeronautics and Astronautics, Nanjing 210016, P. R. China;
2. China Aerodynamics Research and Development Center, Mianyang 621000, P. R. China;
3. Aircraft Strength Research Institute of China, Xi'an 710065, P.R. China

(Received 25 April 2021; revised 10 June 2021; accepted 15 July 2021)

Abstract: This paper discusses the temperature field distribution of piezoelectric stack with heating and thermal insulation device in cryogenic temperature environment. Firstly, the model of the piezoelectric damper is simplified and established by using partial-differential heat conduction equation. Secondly, the two-dimensional Du Fort-Frankel finite difference scheme is used to discretize the thermal conduction equation, and the numerical solution of the transient temperature field of piezoelectric stack driven by heating film at different positions is obtained by programming iteration. Then, the cryogenic temperature cabinet is used to simulate the low temperature environment to verify the numerical analysis results of the temperature field. Finally, the finite difference results are compared with the finite results and the experimental data in steady state and transient state, respectively. Comparison shows that the results of the finite difference method are basically consistent with the finite element and the experimental results, but the calculation time is shorter. The temperature field distribution results obtained by the finite difference method can verify the thermal insulation performance of the heating system and provide data basis for the temperature control of piezoelectric stack.

Key words: thermal differential equation; temperature field; finite difference; piezoelectric stack; heating and thermal insulation device

CLC number: TP391 **Document code:** A **Article ID:** 1005-1120(2021)S-0017-07

0 Introduction

With the continuous development of aircraft, wind tunnel simulation tests require higher Reynolds number simulation capabilities[1]. The cryogenic temperature wind tunnel solves the problem of low Reynolds number in conventional wind tunnels by combining cryogenic temperature technology with wind tunnel technology[2].

The airplane model relies on the tail strut to support the air blowing test in the conventional wind tunnel, and the vibration damper, in the tail strut structure, with the piezoelectric element as the core suppresses the model's vibration. However, due to the large loss of output performance of the piezoelectric element in a cryogenic temperature environment[3], it is necessary to heat the piezoelectric vibration damping joint to ensure its vibration suppression effect. Researchers in NASA Langley Research Center proved that the output performance loss of piezoelectric ceramics was as high as 50% at −150 ℃[3]. Tougher glass fiber and SiO_2 aerosol composite were selected in Refs.[4-6] and the experiment results showed that when the fiber addition

*Corresponding author, E-mail address: m13981192775@163.com.

How to cite this article: CHEN Yixiao, YANG Xinghua, YU Li, et al. Numerical simulation and experimental verification of temperature distribution of piezoelectric stack with heating and thermal insulation device[J]. Transactions of Nanjing University of Aeronautics and Astronautics, 2021, 38(S): 17-23.

http://dx.doi.org/10.16356/j.1005-1120.2021.S.003

was 16%, the thermal conductivity of the composite material was 0.023 2 $W \cdot m^{-1} \cdot K^{-1}$.

This study ensures that the stack works in a suitable temperature range by sticking heaters on the surface of the piezoelectric stack and wrapping the insulation. Therefore, accurate temperature prediction is important for effective operation of piezoelectric vibration damper. As a result, this work is undertaken to study the temperature distribution of the piezoelectric stack[7]. In this paper, the thermal physical models and finite difference model are analyzed to obtain the transient temperature field of piezoelectric vibration damper. The temperature field results can provide reference for the control of the stack temperature and the effect of the vibration damper.

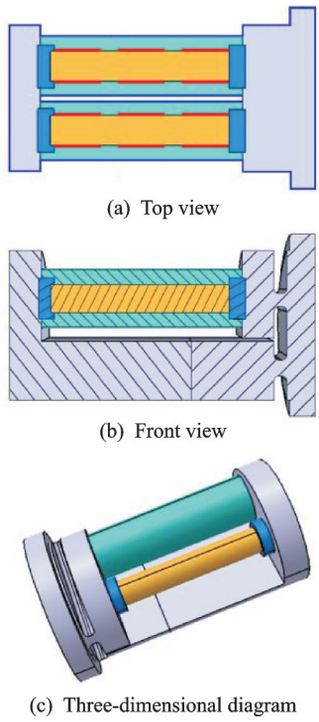

Fig.1 System of piezoelectric damper

1 Model of Heat Conduction System

1.1 Theory and model

The vibration damping joint structure is composed of piezoelectric stack, gaskets, metal structure and insulation. The model of the system is shown in Fig.1. The damper is placed in a cryogenic temperature environment, the heat convection occurs among the surface and the external environment, and the stack is heated by heaters pasted on the surface of the piezoelectric stack. The radius of the piezoelectric stack, the core part of the damping structure, is 5 mm and the length is 56 mm, with ρ=7 800 $kg \cdot m^{-3}$, c=350 $J \cdot kg^{-1} \cdot K^{-1}$ and λ=1.1 $W \cdot m^{-1} \cdot K^{-1}$. Gaskets are installed at both ends of the stack, with the thickness of 5 mm. ZrO_2 is used as the material of the gasket, with ρ=5.85 $kg \cdot m^{-3}$, c=427 $J \cdot kg^{-1} \cdot K^{-1}$ and λ=1.6 $W \cdot m^{-1} \cdot K^{-1}$. The metal part of the vibration damping system uses 304 stainless steel, as ρ=7 930 $kg \cdot m^{-3}$, c=3.5 $J \cdot kg^{-1} \cdot K^{-1}$ and λ=13 $W \cdot m^{-1} \cdot K^{-1}$. Since the thermal conductivity of metal is much bigger than those of the stack and gasket, the influence of the shape of the metal structure on the temperature field distribution of the stack is ignored. Therefore, it is reasonable to simplify the metal part to a cylinder coaxial with the stack. Its radius and height are related to the surface area and volume of the original structure. The insulation is considered adiabatic in this model, as the thermal conductivity is 0.007 $W \cdot m^{-1} \cdot K^{-1}$, which is much smaller compared with others' in the system.

The basic mathematical model of temperature field numerical simulation is Fourier partial differential equation of heat conduction, which is a general equation that the temperature field of all thermally conductive objects should satisfy[8-10]. As the piezoelectric stack, gaskets, and metal structure in this model are all cylindrical, the thermal conductivity differential equation of the transient temperature field in the cylindrical coordinate system is[11-13]

$$\rho c \frac{\partial T}{\partial t} = \lambda \left(\frac{\partial^2 T}{\partial r^2} + \frac{1}{r} \cdot \frac{\partial T}{\partial r} + \frac{\partial^2 T}{\partial z^2} \right) \tag{1}$$

where ρ is the density, c the heat capacity, T the temperature of piezoelectric stack, t the time, λ the thermal conductivity, and r the radius.

1.2 Boundary conditions

The vibration damping joint structure is placed in a cryogenic temperature environment with a temperature of T_f while the piezoelectric stack is required to work at an appropriate temperature to

achieve better output effects. This system uses heaters pasted on both ends and the middle of the piezoelectric stack to realize the temperature control of the stack. The model of the piezoelectric stack is shown in Fig.2, where Ω_1 means the piezoelectric stack, Ω_2 the gasket and Ω_3 the steel structure. U represents the temperature of gaskets and different subscripts are used to distinguish the gaskets at both ends. The heat conduction in the pipe is considered to be two-dimensional heat in the radial and longitudinal directions, and the circumferential heat conduction is ignored[14-16].

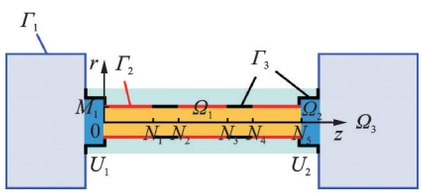

Fig.2 Piezoelectric stack model

The heat transfer inside the model is symmetrical along $r=0$, so the heat transfer needs to be studied when $r\geqslant 0$. As the circumferential heat conduction is ignored in this model, it is considered that there is no heat exchange at the boundary $r=0$.

$$\lambda_1 \cdot \frac{\partial T}{\partial r} = 0 \tag{2}$$

where T is the temperature of the piezoelectric stack[17].

Considering the boundary condition at the interface $r=M_1$, as the surface is pasted with three heaters, the heat is mainly transferred to the piezoelectric stack through three interfaces[18], marked as Γ_2 in Fig.2. Since the stack is wrapped with an insulation, interfaces without heater such as Γ_3 in Fig.2 can be considered as an insulation boundary

$$\lambda_1 \cdot \frac{\partial T}{\partial r} = \begin{cases} q_1 & 0<z<N_1, r=M_1 \\ 0 & N_1<z<N_2, r=M_1 \\ q_2 & N_2<z<N_3, r=M_1 \\ 0 & N_3<z<N_4, r=M_1 \\ q_3 & N_4<z<N_5, r=M_1 \end{cases} \tag{3}$$

The interface $z=0$ and $z=N_5$ are in contact with the gaskets. It is assumed that there is no thermal contact resistance between adjacent media. The energy equation of transient heat conduction at the boundary is

$$\lambda_1 \cdot \frac{\partial T}{\partial z} = \lambda_2 \cdot \frac{\partial U_1}{\partial z} \quad z=0 \tag{4}$$

$$\lambda_1 \cdot \frac{\partial T}{\partial z} = \lambda_2 \cdot \frac{\partial U_2}{\partial z} \quad z=N_5 \tag{5}$$

As the gaskets are wrapped in the insulation, its outer boundary is considered as insulation condition. While metal structure is placed in a cryogenic temperature environment, heat transfer occurs with the fluid through its outer surface, which marked as Γ_1 in Fig.2, according to the Newtonian cooling formula

$$q = h \cdot (T_w - T_f) \tag{6}$$

where T_w and T_f represent the temperature of the wall and fluid, respectively. h is the convective heat transfer coefficient[19]. Since the boundary conditions of the gasket and the metal structure are symmetrical, only the boundary conditions on one side are given. The schematic diagram is shown in Fig.3.

$$\lambda_2 \cdot \frac{\partial U_2}{\partial r} = 0 \quad r=0, 0<z<N_7 \tag{7}$$

$$\lambda_2 \cdot \frac{\partial U_2}{\partial r} = 0 \quad r=M_2, 0<z<N_7 \tag{8}$$

$$\lambda_1 \cdot \frac{\partial T}{\partial z} = \lambda_2 \cdot \frac{\partial U_2}{\partial z} \quad 0<r<M_1, z=0 \tag{9}$$

$$\lambda_2 \cdot \frac{\partial U_2}{\partial z} = 0 \quad M_1<r<M_2, z=0 \tag{10}$$

$$\lambda_2 \cdot \frac{\partial U_2}{\partial z} = \lambda_3 \cdot \frac{\partial \theta_2}{\partial z} \quad 0<r<M_2, z=N_6 \tag{11}$$

$$\lambda_3 \cdot \frac{\partial \theta_2}{\partial r} = 0 \quad r=0, 0<z<N_6 \tag{12}$$

$$\lambda_3 \cdot \frac{\partial \theta_2}{\partial r} = h \cdot (T_w - T_f) \quad r=M_4, 0<z<N_6 \tag{13}$$

$$\lambda_2 \cdot \frac{\partial U_2}{\partial z} = \lambda_3 \cdot \frac{\partial \theta_2}{\partial z} \quad 0<r<M_2, z=0 \tag{14}$$

$$\lambda_3 \cdot \frac{\partial \theta_2}{\partial z} = 0 \quad M_2<r<M_3, z=0 \tag{15}$$

$$\lambda_3 \cdot \frac{\partial \theta_2}{\partial z} = h \cdot (T_w - T_f) \quad M_3<r<M_4, z=0 \tag{16}$$

$$\lambda_3 \cdot \frac{\partial \theta_2}{\partial z} = h \cdot (T_w - T_f) \quad 0<r<M_4, z=N_6 \tag{17}$$

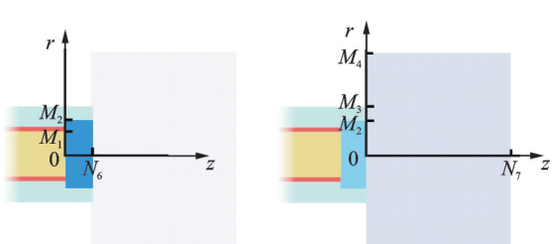

(a) Gasket model (b) Metal structure model

Fig.3 Models of gasket and metal structure

2 Solution Method and Results

Eq.(1) for heat conduction inside the medium is solved by the finite difference method through iterations and two-dimensional method using Du Fort-Frankel explicit difference scheme to discretize and solve the governing equations. Compared with finite element analysis, the finite difference method has the advantages of intuition and short time. Discretized equation is

$$T_{i,j}^{k+1}=\frac{2r+r_0r}{1+4r}T_{i+1,j}^{k}+\frac{2r-r_0r}{1+4r}T_{i-1,j}^{k}+\frac{2r}{1+4r}(T_{i,j+1}^{k}+T_{i,j-1}^{k})+\frac{1-4r}{1+4r}T_{i,j}^{k-1}$$
$$i=1,\cdots,N-1;j=1,\cdots,M-1 \quad (18)$$

$$r_0=\frac{\Delta h}{R} \quad (19)$$

$$r=\frac{\lambda}{\rho c}\cdot\frac{\Delta t}{\Delta h^2} \quad (20)$$

where i, j are the coordinates of the inner node on the z-axis and r-axis; Δh and Δt the space step and time step during the calculation. R is the radius of the cylinder model, ρ the density, c the heat capacity, and λ the thermal conductivity.

Equations of boundary conditions are solve by the central difference approximations during the numerical procedure, substituting differential approximation for derivative

$$\left(\frac{\partial T}{\partial r}\right)_j^k=\frac{1}{2\Delta h}(T_{j+1}^{k}-T_{j-1}^{k}) \quad j=0,M \quad (21)$$

During the programming for numerical computations, the space step are $\Delta r=\Delta z=\Delta h=1$ mm and the time step is $\Delta t=0.1$ ms. The iterative process of the finite difference method is realized by programming, and the data is processed to obtain the transient temperature field of the stack. Fig.4 shows the transient temperature distribution of the piezoelectric stack at an ambient temperature of −70 ℃ and two heating methods. Fig.4(a) is the temperature field distribution of the stack when the heaters pasted on both ends are driven, and Fig.4(b) is the result when the middle heater is working.

It can be found from Fig.4(a) that only when the heating flies at both sides of the stack are working, the temperature on the surface of the stack is unevenly distributed along the axial. Therefore, it is scientific to heat the stack with three evenly distributed heaters.

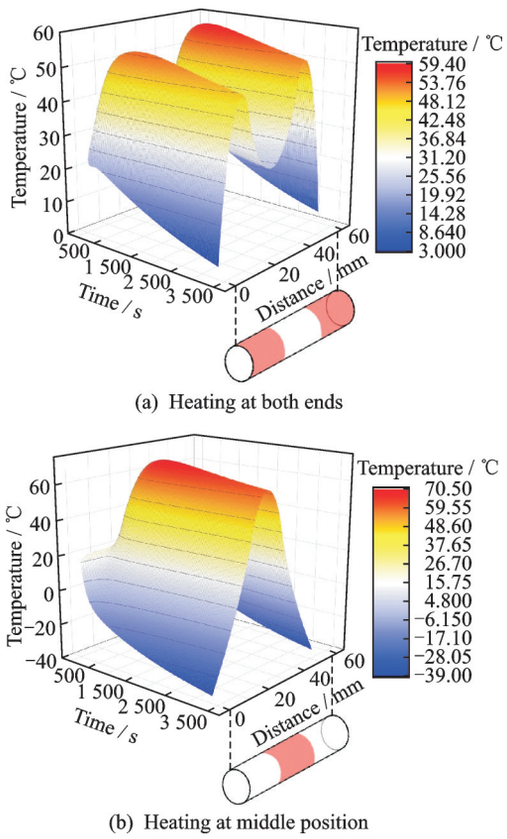

Fig.4 Finite difference transient temperature field

3 Model Identification

In order to verify the temperature field distribution of the stack calculated by the finite difference method, the cryogenic temperature cabinet is used to simulate the cryogenic temperature by the finite element method.

The model established in finite element is similar to the actual model rather than a regular cylinder. The thermal conductivity of the insulation is set to 0.007 $W\cdot m^{-1}\cdot K^{-1}$, and those of other materials are the same as that set in finite difference. The contact mode between different materials is non-separation, and the grid width of the stack surface is 0.5 mm. The ambient temperature of the heat transfer model is set to −70 ℃, and the heat flux density at the heating film is 4 255 W/m^2. Fig.5 gives the comparison results of the finite element method and the finite difference method under two heating conditions. Because of the difference between surface areas of

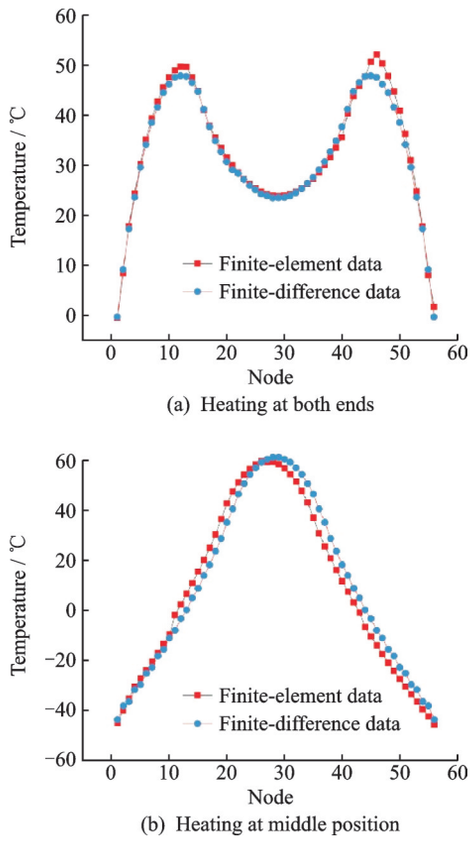

Fig.5 Temperature comparison results between finite element method and finite difference method

the front and rear metal structure in the finite element model, it shows asymmetric results, but the temperature difference is small.

In the experiment, PI piezoelectric stacks, zirconia gaskets and nano-aerogel insulation materials were selected. The piezoelectric vibration damping structure, with heaters attached to both ends and the middle of the stack, was placed in the cryogenic temperature cabinet (Fig.6(a)). The working power of the heaters was maintained at 2 W while the cryogenic temperature cabinet temperature was set to −70 ℃. The temperature sensors were pasted at the position shown in Fig.6(b), measuring the transient temperature. Fig.6(c) shows the stack after wrapping the insulation layer. The installation and placement of the structure are shown in the Fig.6 (d). The test piece taken out from the low temperature cabinet is shown in Fig.6(e).The experimental results are shown in the red curves in Fig.7.

In the experiment, when the structure reaches a steady state, the surface temperature of the metal structure is −60.89 ℃, the gasket temperature is

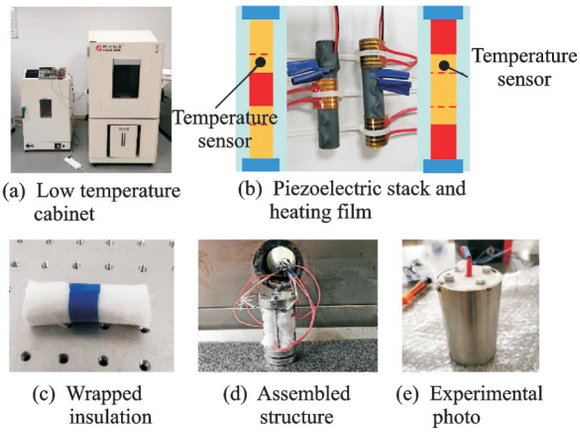

Fig.6 Experiment equipment

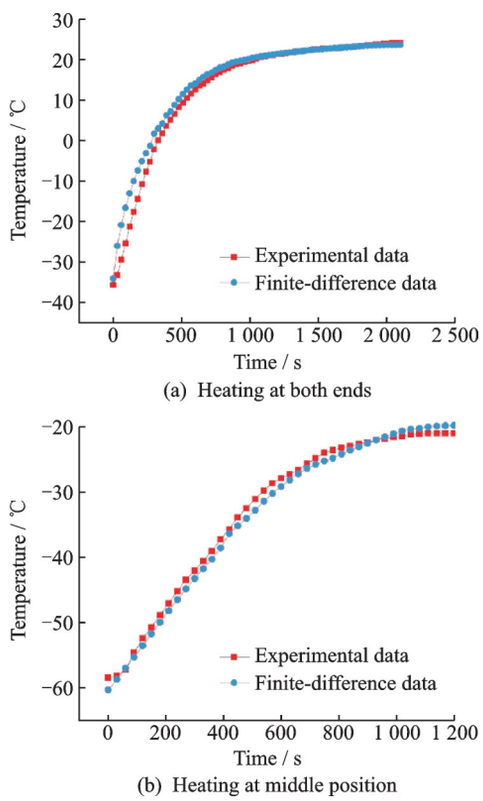

Fig.7 Temperature comparison between finite difference result and experimental data

−16.35 ℃, and the temperature at the stack measurement point is 24 ℃ when the two ends are heated. Correspondingly, according to the calculation result of the finite difference method, the steady state temperatures of the metal surface, the gasket and the measuring point are −63.55, −19.74, and 23.65 ℃, respectively. In another condition when the middle heater is driven, the steady state temperature of the measuring point is −21 ℃ while the calculated data is −19.76 ℃. The comparison between

the finite difference result and the experimental data is shown in the Fig.7.

It can be found from Fig.7 that the temperature response trend calculated by the numerical method is basically consistent with the experimental measurement, but the response curve obtained from the experiment has a certain time lag compared with the numerical simulation result. This is because the heating film has a certain time lag when it is energized to its stable heating.

4 Conclusions

This paper established the thermal conduction model of piezoelectric damping joint, and discretized the partial differential heat conduction equation. Transient temperature response of the piezoelectric stack under different heating modes were obtained and compared with the finite element data. Moreover, experiments in cryogenic temperature cabinet were conducted for verification. The results showed that the maximum error was no more than 4 ℃, and the calculation time was reduced by more than 80% compared with that of the finite element method. The comparison reveals that the finite difference results are consistent with the experimental data closely. Consequently, it is reliable and effective to use the finite difference method to calculate the stack temperature field.

References

[1] BAKER C J, BROCKIE N J. Wind tunnel tests to obtain train aerodynamic drag coefficients: Reynolds number and ground simulation effects[J]. Journal of Wind Engineering and Industrial Aerodynamics, 1991, 38(1): 23-28.

[2] CHEN Z, ZHANG W, GAO R, et al. Theoretical and experimental studies of vacuum cooling of liquid nitrogen[J]. Journal of Aerospace Power, 2019, 34(9): 1971-1976.

[3] MIN C, LUO K, SHAO C, et al. A finite difference discretization method for heat and mass transfer with robin boundary conditions on irregular domains[J]. Journal of Computational Physics, 2019, 400: 108890.

[4] LIU J, ZHU X, CAO X, et al. Experimental research on the influence of natural convection on the flow field in the cabin mockup[J]. Journal of Tianjin University Science and Technology, 2016, 49(3): 221-230.

[5] RYU J. Flexible aerogel superinsulation and its manufacture: US6068882A[P]. 2000-05-30.

[6] XIN S, LIU Z, DING Y, et al. Preparation and application of nano-silica aerogels in thermal insulation: An overview[J]. Materials Review, 2018, 32(5):788-795.

[7] ANGRISANI G, SASSO M, TARIELLO F. Thermo-economic analysis of a solar heating and cooling system with desiccant-based air handling unit by means of dynamic simulations[C]//Proceedings of ASME Biennial Conference on Engineering Systems Design & Analysis. Copenhagen, Denmark: ASME, 2014.

[8] GLUSHKOV D O, KUZNETSOV G V, STRIZHAK P A, et al. Numerical simulation of gel fuel gas-phase ignition by a local source of limited heat content[J]. Acta Astronautica, 2018,163: 44-53.

[9] AVDONIN N A, VOLOKHONSKII L A, IVANOVA G F, et al. Calculation of the temperature field of a bar for hardening in a water-cooled crystallizing tank[J]. Journal of Engineering Physics, 1970, 18(1): 93-99.

[10] LIANG Y, WANG D, GAO L, et al. Calculation of temperature field in power capacitor[J]. IEEE Transactions on Industrial Electronics, 2015, 62(5): 2788-2794.

[11] OBERGUGGENBERGER M, OSTERMANN A. Numerical solution of differential equations[M]. London: Springer, 2011.

[12] DAWES W R J, SHORT D L. The efficient numerical solution of differential equations for coupled water and solute dynamics: the WAVES model: (93/18): 24p. 11 refs, illus[R]. [S.l.]:[s.n.], 1993.

[13] BOTHA J, PINDER G, PATERA A T. Fundamental concepts in the numerical solution of differential equations[J]. Journal of Applied Mechanics, 1983, 51(3): 708.

[14] WAYNER P C, KAO Y K, LACROIX L V. The interline heat-transfer coefficient of an evaporating wetting film[J]. International Journal of Heat and Mass Transfer, 1976, 19(5): 487-492.

[15] HAGISHIMA A, TANIMOTO J. Field measurements for estimating the convective heat transfer coefficient at building surfaces[J]. Building and Environment, 2003, 38(7): 873-881.

[16] YANG X F, YAO K. Uncertain partial differential equation with application to heat conduction[J]. Fuzzy Optimization and Decision Making, 2017, 16(3): 379-403.

[17] YAMAMOTO S. Finite-difference method for heat

conduction equation and excel calculation[J]. Journal of the Technical Association of Refractories, 2008, 28(4): 239-244.

[18] SARAFRAZ M M, PEYGHAMBARZADEH S M. Influence of thermodynamic models on the prediction of pool boiling heat transfer coefficient of dilute binary mixtures[J]. International Communications in Heat & Mass Transfer, 2012, 39(8): 1303-1310.

[19] KUMAR R, VARMA H K, MOHANTY B, et al. Prediction of heat transfer coefficient during condensation of water and R-134a on single horizontal integral-fin tubes[J]. International Journal of Refrigeration, 2002, 25(1): 111-126.

Authors Miss **CHEN Yixiao** received her M. S. degree from Nanjing University of Aeronautics and Astronautics. Her research interests include temperature control system.

Mr. **YANG Xinghua** works in China Aerodynamics Research and Development Center. His research is focused on active vibration control, wind tunnel testing and aerodynamics.

Author contributions Miss **CHEN Yixiao** designed the study, conducted the calculation and analysis, conducted experiment and interpreted the results. Mr. **YANG Xinghua** and Mr. **YU Li** contributed to the discussion and background of the study. Prof. **SHEN Xing** provided the design ideas and experimental equipment conditions, and gave constructive opinions on project research. All authors commented on the manuscript draft and approved the submission.

Competing interests The authors declare no competing interests.

(Production Editor: SUN Jing)

尾支杆减振系统的加热保温系统数值模拟及实验验证

陈逸笑[1,3], 杨兴华[2], 俞　立[2], 沈　星[1]

(1.南京航空航天大学机械机构力学及控制国家重点实验室,南京 210016,中国;
2.中国空气动力研究与发展中心,绵阳 621000,中国; 3.中国飞机强度研究所,西安 710065,中国)

摘要:探讨了低温环境温度下带有加热保温设计的尾支杆减振系统的温度场分布。首先简化并利用偏微分热传导方程建立了减振结构的模型。其次,采用二维Du Fort-Frankel有限差分格式离散化热传导方程,并编程迭代得到了不同位置处加热膜驱动时,压电叠堆瞬态温度场的数值解。然后,利用低温箱模拟低温环境进行实验验证温度场的数值分析结果。最后,将有限差分结果分别与有限元稳态结果和实验瞬态数据进行比较。对比结果表明:有限差分法的结果与有限元、实验结果基本吻合,但所需的计算时间更短,是一种有效的预测其温度场的方法。通过有限差分法获得的温度场分布结果可以验证加热系统的保温性能,并为压电叠堆的温度控制提供数据基础。

关键词:导热偏微分方程;温度场;有限差分法;压电叠堆;加热保温系统